DEVELOPMENT AND VALIDATION OF MRI-DERIVED DETAILED HEAD-NECK FINITE MODEL

Bahreinizad, H., Wei, L.HI, Paulon, G.M., **Chowdhury, S.K.***
Department of Industrial, Manufacturing, and Systems Engineering, Texas Tech University, Lubbock, Texas
*E-mail: suman.chowdhury@ttu.edu

We developed an anatomically accurate detailed head-neck FE model from magnetic resonance imaging (MRI) of soft (muscles, ligaments, brain, etc.) and hard tissues (skull, bones, etc.) of the head-neck system of a male participant (age: 42 years, height: 176 cm, and weight: 235 lbs) using Texas Tech University Neuroimaging Center's 3T MRI scanner [1]. By using MRI modality only, we avoided two image processing challenges: 1) hard (traditionally imaged by using CT scan) and soft (imaged by using MRI scan) tissue coregistration difficulties [2-5], and 2) exposing human subjects to the inherent radiation of the CT scanner [6-8]. Using commercial Mimics 24 and 3-matic software platform (Materialise Inc., USA), we segmented the MRI images and generated high-quality anatomical features of scalp, skull, brain, pia matter, dura matter, cerebrospinal fluid (CSF), cervical bones (C1-C7), and intervertebral. To ensure the accuracy of the articulation and integrity of the vertebral morphology, we performed principal component analysis in MATLAB R2021b program to determine both alignment and orientation of each neck segment. We compared and validated both articulation and morphological data (translational and rotational orientation, height, depth, etc.) of each vertebral bone and intervertebral disc with the literature [9]. To explore the contribution of neck muscles to mechanical loads, we added following neck muscles to the model: Obliquus capitis superior, Superior Longus colli, Rectus capitus major, Rectus capitus minor, Longus capitis, Rectus capitis ant, Rectus capitis lat, Anterior Scalene, Middle scalene, Posterior scalene, Sternocleidomastoid, Longissimus capitis, Longissimus Cervicis, Multifidus cervicis, Semisplenius capitus, Semispinalis cervicis, Splenius capitis, Splenius cervicis, Levator scapula, Oblique capitus inferior and Trapezius. The origin, insertion, and muscle path information were taken from the literature [10]. We also added following neck ligaments as they provide stability to the head and neck complex: anterior longitudinal ligament (ALL), posterior longitudinal ligament (PLL), ligamentum flavum (LF), capsular ligament (CL), interspinous ligaments (ISL), tectorial membrane, anterior and posterior atlanto-occipital ligaments, anterior and posterior atlanto-axial ligaments, Apical ligament, alars ligament, transverse ligament, and Cruciate Ligament of Atlas.

Table 1: Material properties of solid elements of the model

Material	Type	Density [ton/mm^3]	Young modulus [GPa]	Poisson Ratio	Bulk Modulus [GPa]
Bone [11]	Linear elastic	1.2E-9	15.0000	0.22	-
Skin [12]	Linear elastic	1.0E-9	0.01670	0.42	-
Discs [13]	Linear elastic	1.2E-9	0.00480	0.22	-
CSF [14]	Elastic fluid	1.0E-9	0.00131	0.49999	2.1900
Pia mater [12]	Linear elastic	1.0E-9	0.00230	0.45	-
Dura mater [12]	Linear elastic	1.0E-9	0.00500	0.45	-

Due to inherent complexity and irregularities of individual segments, a high-quality mesh was generated to mesh the head-neck geometry. To maintain the quality of the mesh structure, we used 3, 45, 10, and 0.7 as threshold values for aspect ratio, skewness, warping and max angle, respectively. The resulted mesh structures included 1.9 million tetrahedral elements, in which scalp, skull, CSF, brain, vertebrae and intervertebral discs have 0.27, 0.47, 0.33, 0.68, 0.07 million elements, respectively. On the contrary, pia and dura matters were meshed using 81 thousand triangular (shell) elements. Previous biomechanical studies have used a wide range of material properties, ranging from linear elastic to complex non-linear properties, to describe the mechanical response of individual head and neck components [11-21]. We modeled scalp, skull, pia mater, dura mater, intervertebral discs, and vertebrae as linear elastic material and the CSF as solid elements with fluid-like behavior (elastic fluid) [11, 14]. Brain tissue has a very complicated and nonlinear mechanical behavior [22]. So, we modeled the brain as an isotropic homogeneous viscoelastic material [23]. Density, bulk modulus, decay constant, and short-term shear modulus and of the brain were respectively set to 1.06e-9 ton/mm^3, 1.125 GPa, 4.9e-8 GPa, 145, and 1.67e-8 GPa [23]. The material properties of other head-neck structures are provided in Table 1. We used a Hill type muscle model to define both active and passive mechanical behavior of the muscles [24]. Muscle volume and physiological cross section area (PCSA) were taken from the literature [18].

Muscle resting length was calculated as muscle volume divided by the PCSA and the maximum velocity of contracting element was set to 10 times the resting length of a given muscle [24]. Maximum pressure of the muscle was set to 0.3 MPa [24]. We employed *tied contact* to simulate the coupling between discs and vertebrae, skull and scalp, brain and CSF, Skull and dura mater, brain and pia mater and neck-skull articulations. We fixed the bottom of the C7 cervical vertebrae wherein all its degrees of freedom were restricted.

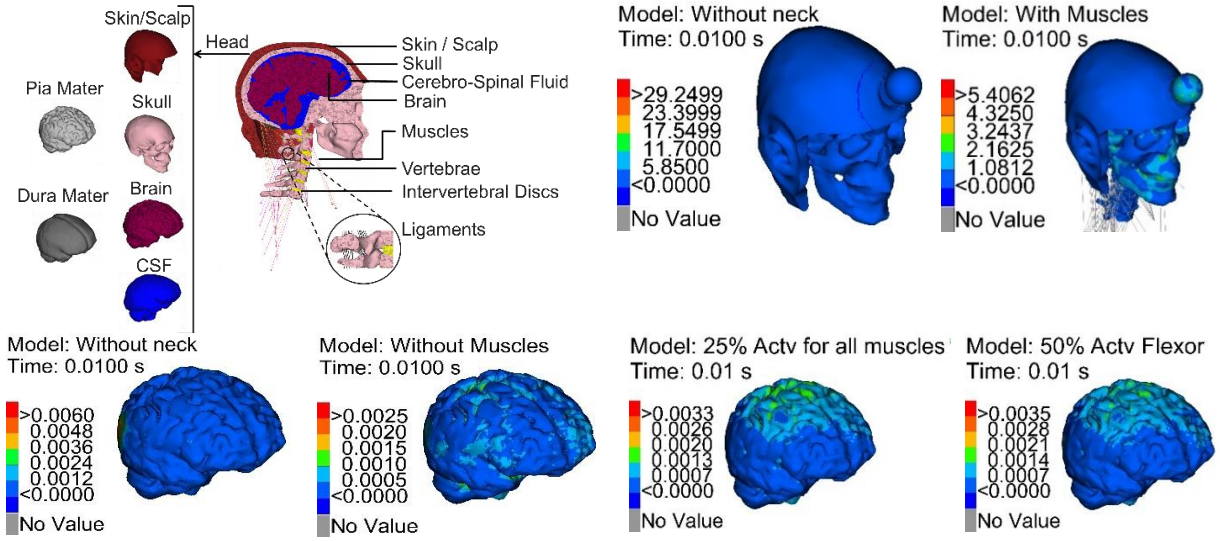

Fig. 1: Our MRI-derived detailed head-neck FE model (top left), preliminary impact tests (top middle and top left), and results (bottom figures). Bottom figures show the von Mises stress contour in the brain for various head-neck modeling scenarios (from left to right); head model, head-neck model, head-neck model with 25% muscle activations, and head-neck model with 50% activation in flexor muscles and 25% muscle activations in extensor muscles.

[1] TTNI. "Texas Tech University Neuroimaging Institute." https://www.depts.ttu.edu/research/ttni/ (accessed July 13, 2022).
[2] B. M. Frye, A. A. Najim, J. B. Adams, K. R. Berend, and A. V. Lombardi Jr, "MRI is more accurate than CT for patient-specific total knee arthroplasty," *The knee,* vol. 22, no. 6, pp. 609-612, 2015.
[3] A. D. Klose *et al.*, "In vivo bioluminescence tomography with a blocking-off finite-difference method and MRI/CT coregistration," *Medical physics,* vol. 37, no. 1, pp. 329-338, 2010.
[4] J. X. Tao, S. Hawes-Ebersole, M. Baldwin, S. Shah, R. K. Erickson, and J. S. Ebersole, "The accuracy and reliability of 3D CT/MRI co-registration in planning epilepsy surgery," *Clinical Neurophysiology,* vol. 120, no. 4, pp. 748-753, 2009.
[5] N. F. Rulkov, I. Timofeev, and M. Bazhenov, "Oscillations in large-scale cortical networks: map-based model," *Journal of computational neuroscience,* vol. 17, no. 2, pp. 203-223, 2004.
[6] J. M. Albert, "Radiation risk from CT: implications for cancer screening," *American Journal of Roentgenology,* vol. 201, no. 1, pp. W81-W87, 2013.
[7] D. J. Brenner and E. J. Hall, "Computed tomography—an increasing source of radiation exposure," *New England journal of medicine,* vol. 357, no. 22, pp. 2277-2284, 2007.
[8] P. W. Wiest, J. A. Locken, P. H. Heintz, and F. A. Mettler Jr, "CT scanning: a major source of radiation exposure," in *Seminars in Ultrasound, CT and MRI*, 2002, vol. 23, no. 5: Elsevier, pp. 402-410.
[9] A. N. Vasavada, J. Danaraj, and G. P. Siegmund, "Head and neck anthropometry, vertebral geometry and neck strength in height-matched men and women," *Journal of biomechanics,* vol. 41, no. 1, pp. 114-121, 2008.
[10] S. Standring, *Gray's anatomy e-book: the anatomical basis of clinical practice*. Elsevier Health Sciences, 2021.
[11] M. Salimi Jazi, A. Rezaei, F. Azarmi, M. Ziejewski, and G. Karami, "Computational biomechanics of human brain with and without the inclusion of the body under different blast orientation," *Computer methods in biomechanics and biomedical engineering,* vol. 19, no. 9, pp. 1019-1031, 2016.
[12] L. Tuchtan, Y. Godio-Raboutet, C. Delteil, G. Léonetti, M.-D. P. Marti, and L. Thollon, "Study of cerebrospinal injuries by force transmission secondary to mandibular impacts using a finite element model," *Forensic science international,* vol. 307, p. 110118, 2020.
[13] J. Z. Wu, C. S. Pan, B. M. Wimer, and C. L. Rosen, "Finite element simulations of the head–brain responses to the top impacts of a construction helmet: Effects of the neck and body mass," *Proceedings of the Institution of Mechanical Engineers, Part H: Journal of engineering in medicine,* vol. 231, no. 1, pp. 58-68, 2017.
[14] K. M. Tse, L. B. Tan, S. P. Lim, and H. P. Lee, "Conventional and complex modal analyses of a finite element model of human head and neck," *Computer methods in biomechanics and biomedical engineering,* vol. 18, no. 9, pp. 961-973, 2015.
[15] R. Willinger, H.-S. Kang, and B. Diaw, "Three-dimensional human head finite-element model validation against two experimental impacts," *Annals of biomedical engineering,* vol. 27, no. 3, pp. 403-410, 1999.
[16] Z. Zong, H. Lee, and C. Lu, "A three-dimensional human head finite element model and power flow in a human head subject to impact loading," *Journal of Biomechanics,* vol. 39, no. 2, pp. 284-292, 2006.
[17] J. B. Fice, D. S. Cronin, and M. B. Panzer, "Cervical spine model to predict capsular ligament response in rear impact," *Annals of biomedical engineering,* vol. 39, no. 8, pp. 2152-2162, 2011.

[18] M. B. Panzer, J. B. Fice, and D. S. Cronin, "Cervical spine response in frontal crash," *Medical engineering & physics,* vol. 33, no. 9, pp. 1147-1159, 2011.
[19] V. Dirisala, G. Karami, and M. Ziejewski, "Effects of neck damping properties on brain response underimpact loading," *International Journal for Numerical Methods in Biomedical Engineering,* vol. 28, no. 4, pp. 472-494, 2012.
[20] H. Mao *et al.*, "Development of a finite element human head model partially validated with thirty five experimental cases," *Journal of biomechanical engineering,* vol. 135, no. 11, p. 111002, 2013.
[21] E. Boccia, A. Gizzi, C. Cherubini, M. Nestola, and S. Filippi, "Viscoelastic computational modeling of the human head-neck system: Eigenfrequencies and time-dependent analysis," *International Journal for Numerical Methods in Biomedical Engineering,* vol. 34, no. 1, p. e2900, 2018.
[22] S. Budday *et al.*, "Mechanical characterization of human brain tissue," *Acta biomaterialia,* vol. 48, pp. 319-340, 2017.
[23] H.-S. Kang, R. Willinger, B. M. Diaw, and B. Chinn, "Validation of a 3D anatomic human head model and replication of head impact in motorcycle accident by finite element modeling," *SAE transactions,* pp. 3849-3858, 1997.
[24] J. M. Winters, "Hill-based muscle models: a systems engineering perspective," in *Multiple muscle systems*: Springer, 1990, pp. 69-93.